

ELASTIC-PLASTIC BEHAVIOUR OF ADVANCED ADI STUDIED BY IN-SITU SEM TENSILE TEST

Martin PETRENEC ^a, Hana TESAŘOVÁ ^a, Karel KRAHULA ^b, Jaroslav POLÁK ^c

^a TESCAN, a.s., Libušina třída 21, Brno-Kohoutovice, 623 00, Czech Republic, EU,
martin.petrenec@tescan.cz

^b Institute of Physics of Materials of the Academy of Sciences of the Czech Republic, v. v. i., Žižkova 22,
Brno, 616 62, Czech Republic, EU, krahula@ipm.cz

^c CEITEC IPM AS CR, v.v.i., Žižkova 22, 616 62 Brno, Czech Republic, EU, polak@ipm.cz

Abstract

In-situ SEM tensile tests at room temperature have been performed on flat specimen of advanced austempered ductile cast iron (ADI) alloyed with nickel with the aim to study elastic-plastic behavior together with the nucleation and growth of cracks. During tensile loading the systematic observation of selected locations was studied. The in-situ observation was used to elucidate the tensile curves in agreement with the deformation mechanisms. In the early stage of loading the stress-strain response is elastic. After exceeding elastic limit decohesion of graphite nodules from the matrix was observed. It can be related to the departure of the tensile curve from the elastic behavior. The cracks initiated preferably from interface of graphite nodule and the ausferrite matrix. Elastic-plastic region is connected with the plastic deformation of the matrix and growth and linking of short cracks. The tensile curves from in-situ stage and standard tensile test were compared and discussed.

Keywords: ADI with nickel alloying, in-situ tensile test; mechanical properties, deformation mechanisms, SEM-FEG

1. INTRODUCTION

Ductile cast iron is a structural material employed in many industrial applications. Its resistance to fracture in static and cyclic loading is subject of numerous research activities. The mechanical properties of ductile cast iron are similar to those of cast steels. Therefore it is often used for the production of bulky vehicle components. Vehicle components are often subjected to variable loading at depressed temperatures. It is important to choose the optimum structure and evaluate resulting mechanical properties in conditions close to the service conditions [1].

One way to improve the mechanical properties of cast iron represent the changes in chemical composition, e.g. by alloying with nickel. The addition of nickel leads to the improvement of tensile strength and ductility mainly at low temperatures [1-3]. The principal damage mechanism in ductile cast iron is often identified as void growth corresponding to graphite nodules. Numerous studies provided analytical laws to describe the growth of a single void, depending on the void geometry and matrix behavior [4-6]. It is known that the role of graphite nodules in microcrack initiation and propagation is not clear and that the effect of microstructure should be more deeply investigated, namely the effect of Ni alloying. Recent on in-situ studies in scanning electron microscope of austempered ductile cast iron (ADI) or ferritic ductile cast iron were focused only to basic deformation mechanisms and the influence of the matrix [5, 6]. Data focused on the effect of alloying are not available.

The aim of this paper is to study the elastic-plastic behavior together with nucleation and growing of cracks of advanced austempered ductile cast iron alloyed with nickel using in-situ SEM tension test.

2. EXPERIMENTAL DETAILS

2.1 Material and heat treatment

Flat specimen with geometry shown in **Fig. 1a** had rectangular cross section of 1.4 x 1.25 mm² and a gauge length of 2 mm. They were prepared by electro-erosion spark machining from cast 1 kg Y block. Chemical composition is shown in **Table 1**. Specimen surface was carefully grinded and mechanically polished for in-

situ observations and for the analysis of size, the morphology and the fraction of graphitic nodules using image analysis. Results are presented also in **Table 1**. Specimens from ADI were subsequently heat treated under optimum conditions: austenitization annealing at 840 °C /1 hour and isothermal transformation at 375°C (austempering temperature) for 45 minutes with air cooling. Microstructure of the material is shown in **Fig. 2** and **Fig. 3**. It consists of spherical graphite and the matrix, which contains fine bainitic needles and the retained austenite A_r . Volume fraction of retained austenite was determined using neutron diffraction and its typical value is 30 % [7]. The nickel alloying affects the size of nodule diameter (see **Table 1**). The tensile properties have following values: 0.2 % proof strength is equal to 728 MPa, ultimate tensile strength is equal to 1016 MPa and elongation to fracture is equal to 15.6 % [2, 3, 7].

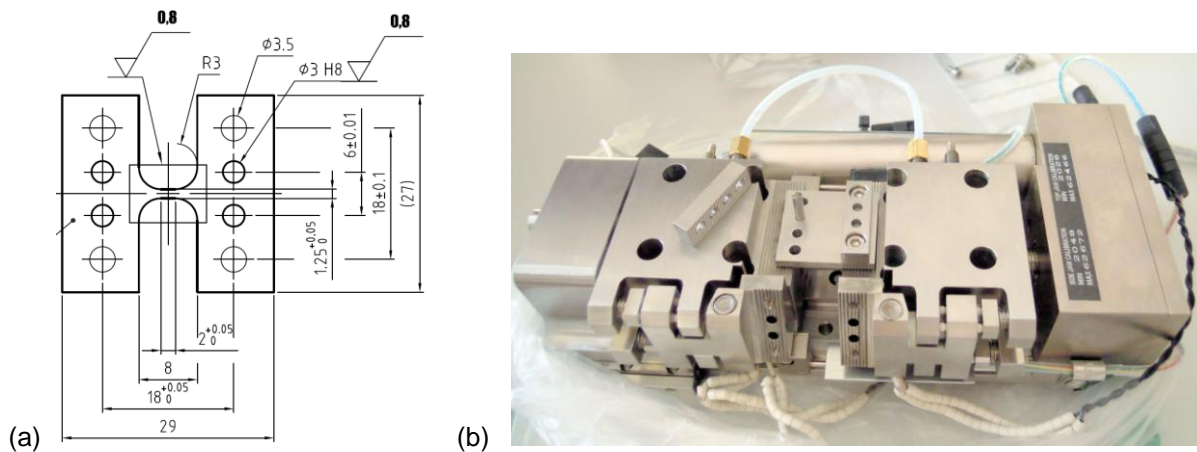


Fig. 1 (a) Specimen geometry for in-situ tension test and (b) the Microtest™ 2000EW with EH 2000 heated grips tensile loading.

Tab. 1 Chemical composition (in wt. %) and nodule characteristics of ductile cast iron [2, 7].

C	Mn	Si	P	S	Cu	Cr	Ni	Mg	Fe	Nodule count (mm ⁻²)	Nodule Area fraction (%)	Nodule diameter (μm)	Nodularity (%)
3.41	0.18	2.35	0.02	0.02	0.02	0.01	2.75	0.05	rest	566	9.53	20.58	92.5

2.2 In situ tensile test

The specimen was tested in-situ in the vacuum chamber of a scanning electron microscope TESCAN MIRA 3 with FEG cathode using GATAN stage Microtest™ 2000EW with EH 2000 heated grips tensile loading stage. The tensile test was performed in force control mode with the motor velocity 0.1 mm/min at room temperature. The extension of jaws was measured by the extensometer mounted on the back side of the stage (**Fig. 1b**). During in-situ deformation SEM micrographs were taken using the four quadrant back-scatter-electron (BSE) and secondary-electron (SE) detectors. And the systematic observation of ten selected locations (in central and in border sections of the specimen). The images were taken for a set values of engineering stress corresponding to the tensile stresses 0, 440, 550, 714, 879, 905, 976, 1016 MPa and after final fracture.

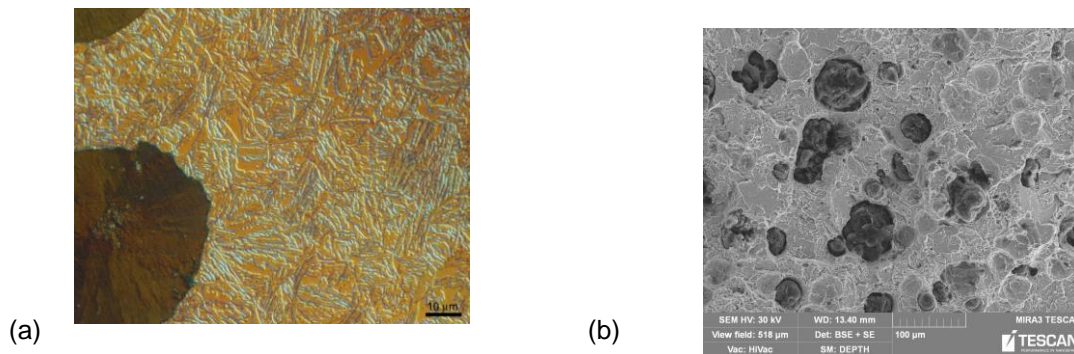


Fig. 2 (a) Optical micrograph and (b) SEM-BSE images of microstructure (b) [2, 7].

3. RESULTS AND DISCUSSION

The macroscopic view of the specimen surface before and after the tensile test shows **Fig. 3**. It demonstrates that the geometry arrangement of the specimen and the stage is axial and the final fracture appeared in the central part of the specimen without the effect of any bending effects. The tensile curve of ADI alloy is shown in **Fig. 4a**. Where the arrows mark the locations when the straining was interrupted for observation of the specimen surface. The interruption produced characteristic relaxation effects. In the early stage of loading the stress-strain response is purely elastic (the proportional elastic limit is approximately 200 MPa). This region has been fitted using linear regression function and the modulus of elasticity (corresponding to the dashed line in **Fig. 4a**) was evaluated. The same proportional elastic limit of ADI alloy was measured on standard cylindrical specimens using servohydraulic machine [7]. After exceeding the elastic limit the departure of the tensile curve from the pure elastic behavior was shown. Macroscopically the material is still in elastic region and only after exceeding the macroscopic yield stress (approximately 890 MPa) the material was in elastic-plastic region. Further increase of the stress lead to final fracture by joining pore defects.

The characteristic example of microstructural observations during in-situ tensile test shows **Fig. 5**. In the pure elastic region the images of graphite and matrix phases do not change in comparison to the original state (**Fig. 5a**). After exceeding elastic limit, the departure of the tensile curve from the pure elastic behavior is connected with the decohesion of graphite nodules from the matrix. This was observed mainly at the edges of the phase graphite/matrix interfaces (see **Fig. 5b,c,d**) where the stress concentration factor is high. The cracking of graphite nodules and progressing decohesion due to the localized deformation of the matrix was observed mainly at the stress exceeding the yield stress (see **Fig. 5e,f**) and in the domain of appreciable plastic deformation (**Fig. 5g,h,i**). In elastic-plastic region the described mechanisms occurred at remaining graphite/matrix interfaces. The cracks initiated preferably from interface of graphite nodule and the ausferrite matrix (see **Fig. 5i**). The end of the elastic-plastic region is connected with the plastic deformation of the matrix and growth and linking of short cracks (**Fig. 4b**). During loading in elastic-plastic region the steadily growing stress is also due to strain induced phase transformation of retained austenite to the ferrite in the matrix, mainly around the deformed graphite nodules. The neutron diffraction study [7] reported the decrease of retained austenite after tensile loading of ADI alloy to 9 %.

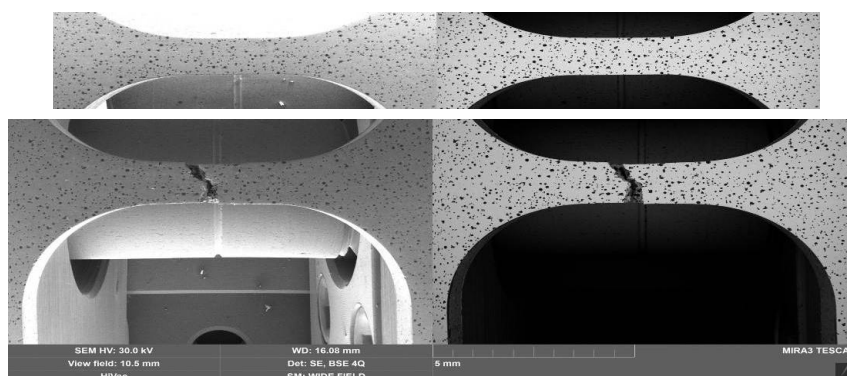
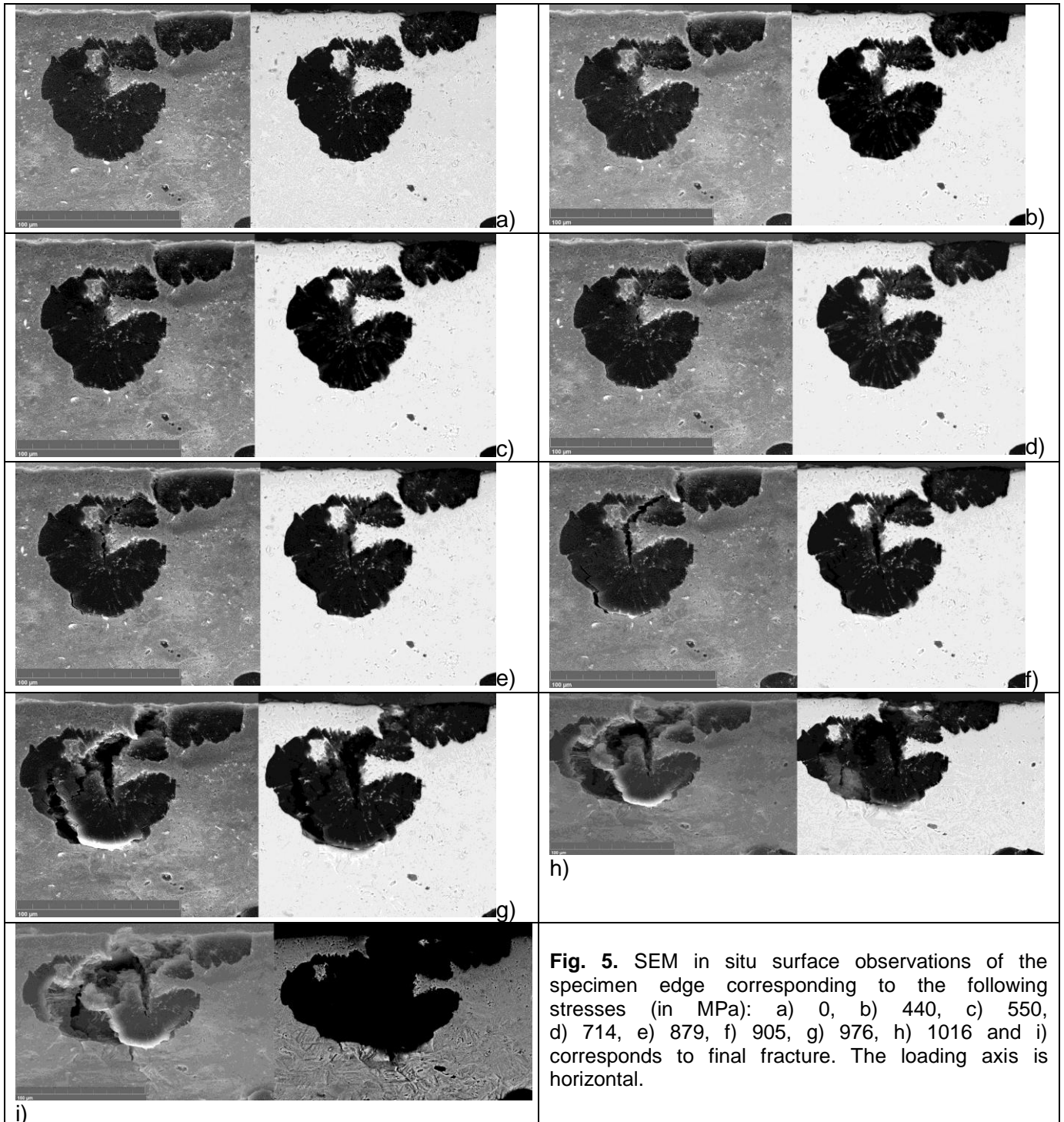
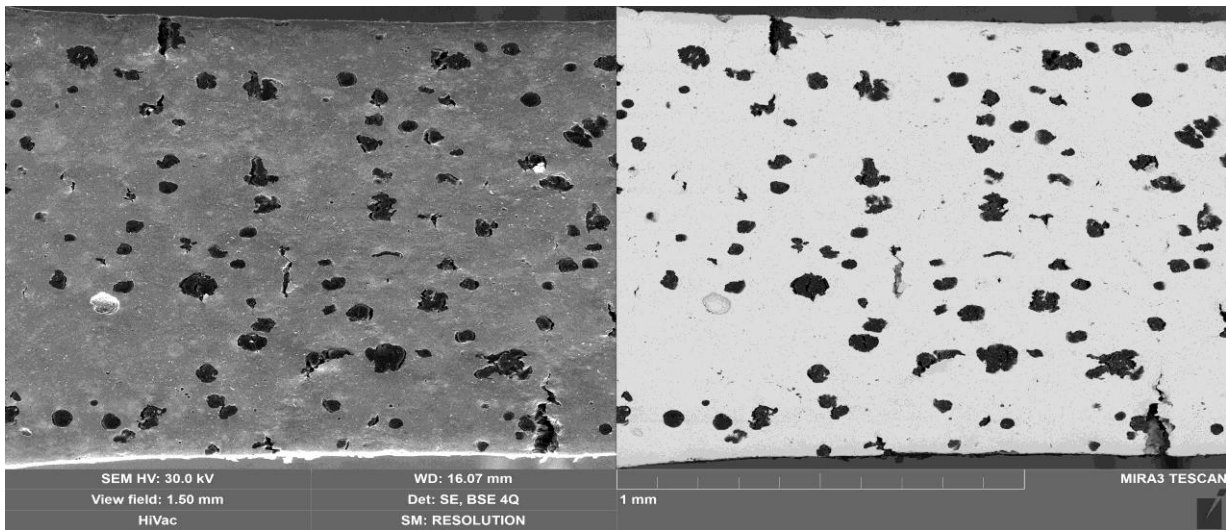
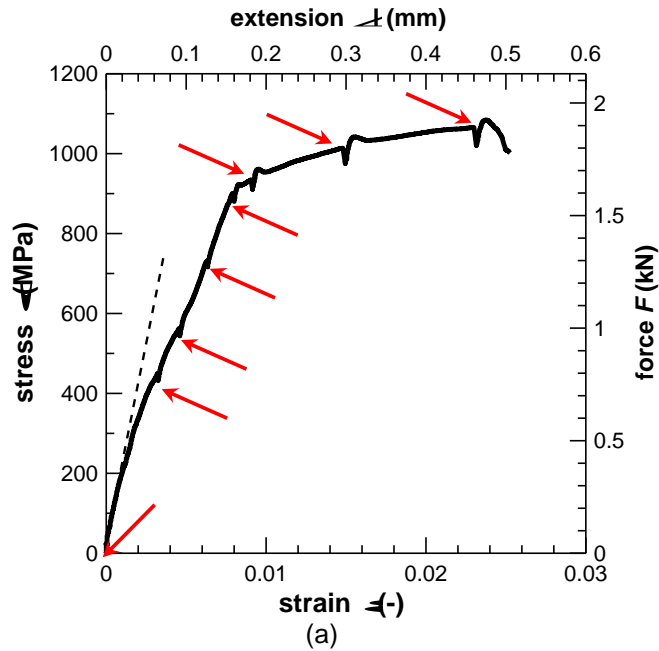


Fig. 3 Specimen surface before (upper image) and after (lower image) tensile test.





(b)

Fig. 4. (a) The tensile curve of ADI alloy (the arrows show interruptions necessary for observation); (b) in-situ image of the specimen surface at the stress 1016 MPa.

4. CONCLUSIONS

The experimental in-situ SEM tensile tests of advanced austempered ductile cast iron (ADI) alloyed with nickel, and their analyses allow to draw following conclusions:

- (i) important details of the deformation mechanisms during tensile straining of ADI can be revealed by GATAN stage and microscope SEM-FEG MIRA 3.
- (ii) the effect of nickel alloying lead to structure refinement and results in the increase of proportionality limit preferably due to lower effect of the notch effect of the graphite.
- (iii) the departure of the tensile curve from the elastic behavior is due to the decohesion of graphite nodules from the matrix. The macroscopic transition from formally elastic to plastic region is connected with cracking of graphite nodules and the plastic deformation of matrix.
- (iv) in the elastic-plastic region the cracks initiate preferably from graphite/matrix phase interface grow and finally link in forming macroscopic crack leading to fracture.

ACKNOWLEDGEMENT

The support by the projects RVO: 68081723 and CEITEC No. CZ.1.05/1.100/02.0068 is gratefully acknowledged.

LITERATURE

- [1] DORAZIL, E. *Austempered ductile iron*. 1. Vyd. Praha: Academia, 1991. 436 s.
- [2] PETRENEC, M., BERAN, P., DLUHOŠ, J., ZOUHAR, M., ŠEVČÍK, M. Analysis of fatigue crack initiation in cycled austempered ductile cast irons. *Procedia Engineering*, 2010, vol. 2, pp 2337–2346.
- [3] PETRENEC, M., TESAŘOVÁ, H., BERAN, P., ŠMÍD, M., ROUPCOVÁ, P. Comparison of low cycle fatigue of ductile cast irons with different matrix alloyed with nickel. *Procedia Engineering*, 2010, vol. 2, pp 2307–2316.
- [4] KOHOUT, J. A simple relation for deviation of grey and nodular cast irons from Hooke's law. *Materials Science and Engineering A313*, 2001, p. 16–23.
- [5] IACOVIELLO, F., BARTOLOMEO, O. Di., COCCO, V. Di, PIACENTE, V. Damaging micromechanisms in ferritic–pearlitic ductile cast irons. *Materials Science and Engineering A*, 2008, Vol. 478, pp 181–186.
- [6] DAI, P.Q., HE, Z.R., ZHENG, C.M., MAO, Z.Y. In-situ SEM observation on the fracture of austempered ductile iron. *Materials Science and Engineering A*, 2001, Vol. 319–321, pp 531–534.
- [7] TESAŘOVÁ, H. Structural and mechanical characteristics of nickel-alloyed ductile cast iron. Ph.D. Thesis, Brno University of Technology; 2009, s. 123.